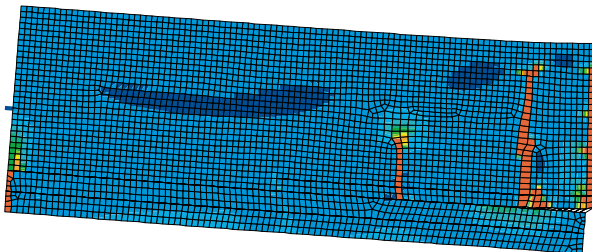
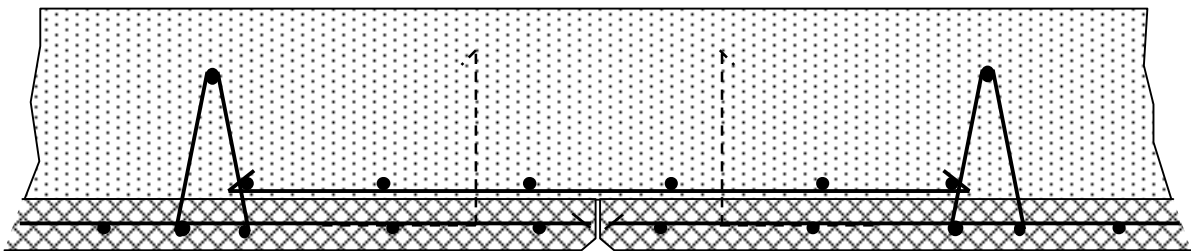


# CHALMERS



## Analyses of a lap splice in a lattice girder system

KARIN LUNDGREN

*Department of Structural Engineering and Mechanics*  
*Concrete Structures*  
CHALMERS UNIVERSITY OF TECHNOLOGY  
Göteborg, Sweden 2003

Report No. 03:3



REPORT NO. 03:3

# Analyses of a lap splice in a lattice girder system

KARIN LUNDGREN

Department of Structural Engineering and Mechanics  
Concrete Structures  
CHALMERS UNIVERSITY OF TECHNOLOGY  
Göteborg, Sweden 2003

Analysis of a lap splice in a lattice girder system

KARIN LUNDGREN

© KARIN LUNDGREN, 2003

ISSN 1651-9035

Report no. 03:3

Department of Structural Engineering and Mechanics

Concrete Structures

Chalmers University of Technology

SE-412 96 Göteborg

Sweden

Telephone: + 46 (0)31-772 1000

Cover:

Example of a lap splice in a lattice girder system, together with crack pattern obtained in a finite element analysis.

Department of Structural Engineering and Mechanics  
Göteborg, Sweden 2003

Analysis of a lap splice in a lattice girder system  
KARIN LUNDGREN  
Department of Structural Engineering and Mechanics  
Concrete Structures  
Chalmers University of Technology

## ABSTRACT

To enable load-carrying in two directions in lattice girder systems, transverse reinforcement is needed. In the present study, the possibility to put transverse reinforcement in the precast concrete panels and complement with lapped reinforcement across the joints at the construction site was studied. The behaviour of such a joint, when subjected to bending, was investigated in two-dimensional finite element analyses.

The analyses show that the cast joint between the precast concrete and the in-situ cast concrete is the weak link in this detailing, as could be expected. In the analyses where a rather large amount of transverse reinforcement was used,  $\varnothing 8$  s150 NPs 700, the joint could be loaded close to yielding of the reinforcement; then opening of the cast joint occurred in all of the analyses. When no bent reinforcement, crossing the cast joint, is present, the failure mode will most likely become brittle. It is therefore recommended to have bent reinforcement crossing the cast joint. Two analyses were carried out with two different placement of bent reinforcement,  $\varnothing 8$  s150 B500B in both cases. When the bent reinforcement was placed close to the joint, it obtained large stresses rather early in the analysis, and the analysis became unstable for rather low rotations. When the bent reinforcement was placed further away from the joint, the transverse reinforcement reached yielding, and the deformation capacity was approximately doubled compared to the other analyses.

For small amounts of transverse reinforcement, or reinforcement with a lower yield strength, it might be possible to use the studied detailing even without bent reinforcement crossing the joint. In one analysis where the transverse reinforcement had a reduced yield strength, 500 MPa instead of 700 MPa, the reinforcement reached yielding, and it was possible to keep the yielding moment some additional rotation before the joint opened up.

The modelling of the cast joint is of very large importance for the results of the analyses. The modelling of that was checked through analyses of joints between precast and in-situ concrete tested by Nissen *et al.* (1986), who made a large experimental investigation on the interaction between precast and in-situ concrete. Still some uncertainty about the input parameters remain. Furthermore, long term effects such as shrinkage and creep were not included in these analyses. It is recommended to do further studies, including full-scale testing of lap splices before this detailing is used in practice.

Key words: Lap splice, lattice girder systems, joint cast, non-linear finite element analyses

Analys av en armeringsskarv i ett plattbärlag

KARIN LUNDGREN

Institutionen för konstruktion och mekanik

Betongbyggnad

Chalmers tekniska högskola

## SAMMANFATTNING

För att möjliggöra bäring i två riktningar i plattbärlag kan bjälklagen armeras i underkanten tvärs huvudsakliga bärriktningen. Denna armering kompletteras sedan med skarvarmering på byggplatsen, som läggs över skarv mellan enskilda plattbärlag. I denna studie har beteendet hos en sådan skarv när den belastas i böjning studerats i tvådimensionella finita elementanalyser.

Analyserna visar att gjutfogen mellan prefab-betongen och den platsgjutna betongen är en svag länk i detta detaljutförande, som kan förväntas. I analyser med en ganska stor andel armering,  $\varnothing 8$  s150 NPs 700, kunde skarven belastas nära till flytning i armeringen, därefter öppnades gjutfogen upp i alla analyserna. När där inte finns någon tvärrarmering över gjutfogen, blir det sannolikt ett sprött brott. Därför rekommenderas ett utförande med tvärrarmering över gjutfogen. Två analyser utfördes med två olika placeringar av uppbockad armering,  $\varnothing 8$  s150 B500B i båda fallen. När tvärrarmeringen var placerad nära fogen erhöll den höga spänningar tidigt i analysen, och analysen blev instabil redan vid ganska låga rotationer. När tvärrarmeringen var placerad längre in från fogen, uppnådde man flytning i armeringen i fogen, och rotationskapaciteten var ungefär dubbelt så stor som i de andra analyserna.

För låga mängder armering, eller armering med en lägre hållfasthet, kan det vara möjligt att använda det studerade utförandet till och med utan tvärrarmering i gjutfogen. I en analys där armeringen hade lägre hållfasthet, 500 MPa i stället för 700 MPa, uppnådde armeringen flytgränsen, och det var möjligt att bära flytmomentet under ytterligare deformationsökning innan gjutfogen öppnades upp.

Hur gjutfogen modelleras har mycket stor betydelse för analysresultaten. Modellen för gjutfogen kontrollerades genom att försök på fogar som utförts av Nissen *et al.* modellerades. Det finns dock fortfarande en del osäkerheter kring indata-parametrar för gjutfogen. Dessutom är långtidseffekter som krypning och krympning inte beaktade i dessa analyser. Ytterligare studier, inkluderande fullskale-försök på skarvar, rekommenderas därför innan detta utförande används i praktiken.

Nyckelord: Armeringsskarv, plattbärlag, gjutfog, icke-linjära finita elementanalyser

# Contents

1	INTRODUCTION	1
2	FINITE ELEMENT MODEL OF A LAP SPLICE IN A LATTICE GIRDER SYSTEM	2
2.1	Modelled geometry	2
2.2	Material	4
2.2.1	Concrete	4
2.2.2	Reinforcement	5
2.2.3	Interaction between concrete and reinforcement	5
2.2.4	Interaction between precast and in-situ cast concrete	6
3	FINITE ELEMENT ANALYSES OF JOINTS BETWEEN PRECAST AND IN-SITU CONCRETE	9
3.1	Finite element models	9
3.2	Calibration of the parameters of the joint	12
4	RESULTS OF ANALYSES OF A LAP SPLICE IN A LATTICE GIRDER SYSTEM	15
4.1	Normal case	15
4.2	With lower values of the cohesion and the coefficient of friction	19
4.3	With higher values of the cohesion and the coefficient of friction	20
4.4	Without considering the welds in the reinforcement mesh	21
4.5	With bent reinforcement crossing the cast joint	24
4.6	With bent reinforcement crossing the cast joint close to the joint	26
4.7	With lower yield strength of the reinforcement	29
4.8	Without welds and with lower yield strength of the reinforcement	30
5	CONCLUSIONS	32
6	REFERENCES	34



## **Preface**

In this study, finite element analyses of lap splices in a lattice girder system were carried out. The analyses were carried out from April 2003 to June 2003. The project was initiated and financed by “Svenska Fabriksbetongföreningens plattbärlagsgrupp”. I would like to thank Ingemar Löfgren for interesting discussions about the studied problem, and for reading and commenting this report.

Göteborg June 2003

Karin Lundgren



# 1 Introduction

The lattice girder system is a semi-precast element floor, where precast concrete panels are combined with in-situ concrete topping, see Figure 1. Lattice girder systems can either be load-carrying in only one direction, or in two directions. To enable load-carrying in two directions, there are two possibilities:

1. Transverse reinforcement is placed on the precast concrete panels on the construction site. The transverse reinforcement bars must then be pulled through the lattice girders, which is time-consuming.
2. The second alternative is to put transverse reinforcement in the precast concrete panels. This must be complemented with lapped reinforcement across the joints at the construction site.

In the work presented here, the second alternative is investigated. An example of such a splice is shown in Figure 2. The aim with this study is to investigate the behaviour and capacity of a joint where the spliced reinforcement consists of mesh between the lattice girder trusses, both with and without bent reinforcement crossing the cast joint as shown in Figure 2. This is done through non-linear finite element modelling.

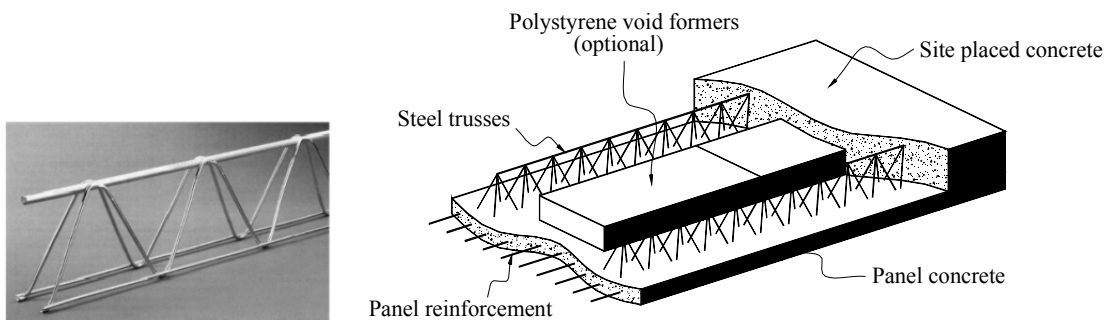


Figure 1 A lattice girder truss and a lattice girder element.

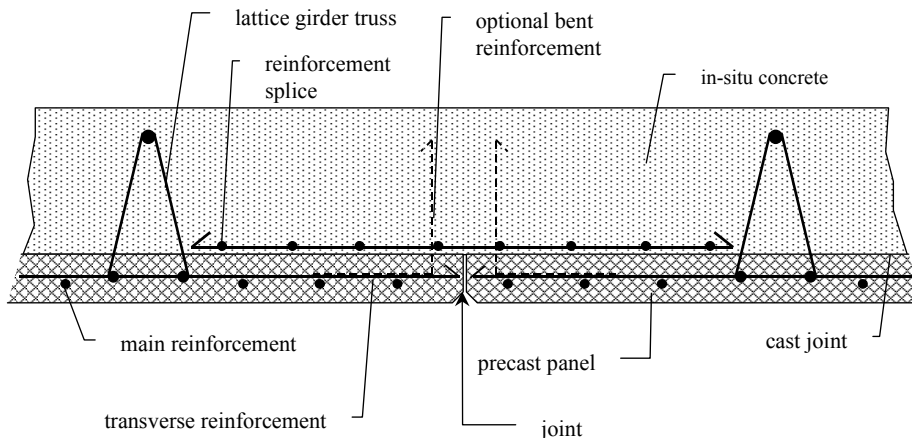


Figure 2 Example of a splice in the joint between two lattice girder elements.

## 2 Finite element model of a lap splice in a lattice girder system

### 2.1 Modelled geometry

A part of a lattice girder system was modelled, using the finite element program Diana version 8.1. The geometry and reinforcement arrangement was chosen as shown in Figure 3. The main reason for the choices of the geometry was what is normally in use. The amount of transverse reinforcement was chosen to be in the upper range of what is in use, as the larger capacity of the transverse reinforcement, the more likely it becomes that other failure mechanisms will become limiting than yielding of the reinforcement.

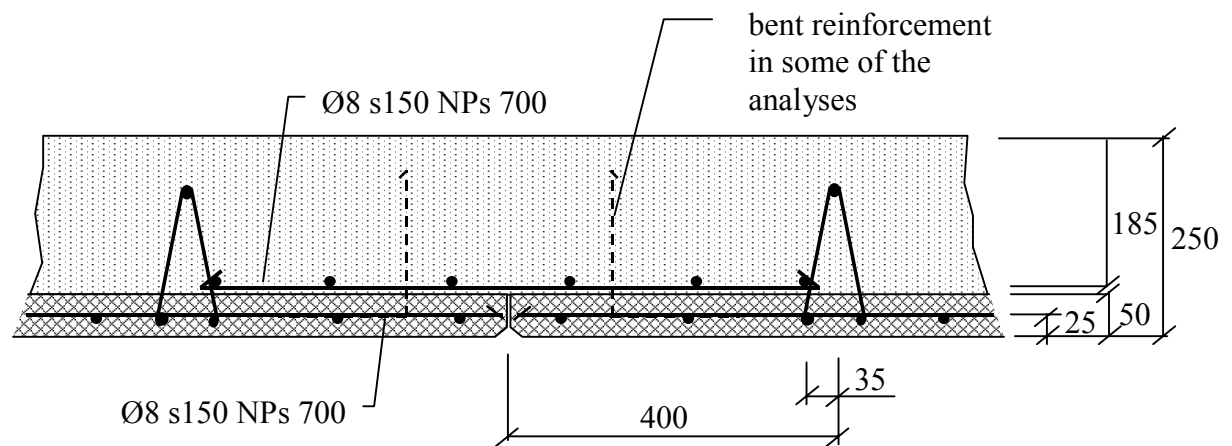


Figure 3 Modelled joint between two lattice girder elements.

Two-dimensional modelling was used, assuming plane stress. The geometry of the modelled part is shown in Figure 4. The symmetry line at the joint between two lattice girder elements was used. Only 700 mm of the plate was modelled; at that distance away from the joint a plane section was assumed, and a bending moment was applied. The concrete was modelled with four-node quadrilateral elements. The transverse reinforcement was modelled with truss elements. Special interface elements were used between the concrete and the reinforcement, describing a bond-slip relation. Also the cast joint was modelled by the use of interface elements, with separate nodes for the precast and the in-situ cast concrete, see Figure 4. The welds in the mesh reinforcement were modelled in such a way that the reinforcement and the concrete nodes were tied to each other at the location of the welds, see Figure 4. This was the only effect of the main reinforcement that was included in the model.

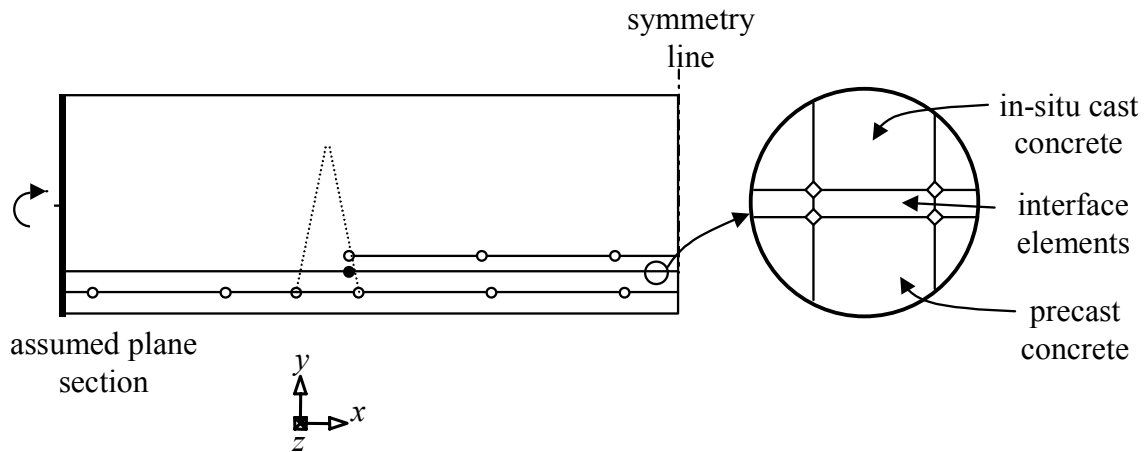


Figure 4 Geometry of the modelled part. The white circles mark where the nodes of the reinforcement and the concrete were tied to each other; the filled circle mark where the nodes of the precast concrete and the in-situ concrete were tied to each other.

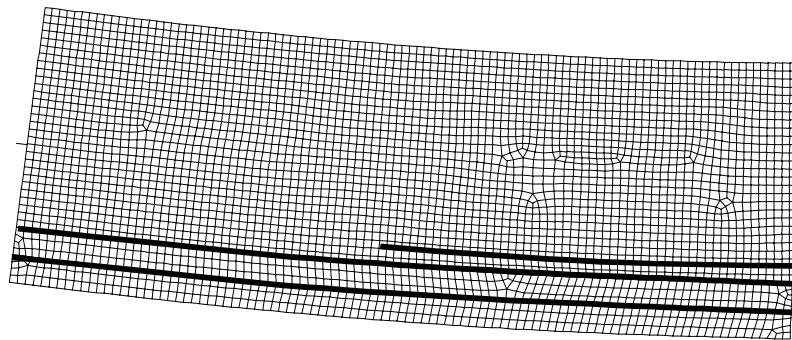


Figure 5 Deformed finite element mesh. The thick lines show the reinforcement and the cast joint.

The effect of the lattice girder trusses was taken into account by tying the nodes of the precast concrete and the in-situ concrete to each other at the location of the centre of the lattice girder truss. In reality, the lattice girder truss provides a more diffuse locking over some distance, and the cast joint is not totally prevented from opening. However, in order not to obtain too complicated models, this modelling technique was chosen. Note that this modelling might lead to an overestimation of the capacity.

In some of the analyses, the effect of bent reinforcement crossing the interface between the precast and the in-situ cast concrete was included. Beam elements were used to model the bent reinforcement, with a circular cross-section. Also for this reinforcement, interface elements were used between the concrete and the reinforcement, describing a bond-slip relation. At the cast joint, very short beam elements were used. The modelling method is further described and discussed in section 3.1.

Some limitations in the modelling are worth discussion. First of all, the stresses in the main direction are not included, since two-dimensional modelling was chosen. Bending in the main direction will affect the studied lap splice in two ways:

- 1) The interface between the precast and the in-situ cast concrete will be used for shear transfer also in the main direction. This will reduce the possibility to transfer shear in the studied direction. This is an important aspect, which most likely needs to be more studied.
- 2) Cracking due to bending in the main direction will affect the bond mechanism between the reinforcement and the concrete in the studied lap splice. This might be important for bars, but when reinforcement meshes is used, most of the anchorage is taken by the welds in the mesh. Then this effect on the bond mechanism is not so important for the splice.

Furthermore, long-term effects such as creep and shrinkage are not included in the modelling. Shrinkage might cause cracking of the in-situ-cast concrete over the joint even before the structure is loaded. However, this might not have any larger influence on the behaviour for larger loads. As the prefabricated concrete and the concrete cast in situ have different ages, the difference in shrinkage will cause stresses in the cast joint. Furthermore, as some parts of the cast joint will be subjected to sustained tensile loading, creep effects in the cast joint might be of importance.

## 2.2 Material

### 2.2.1 Concrete

The concrete was modelled with a constitutive model based on non-linear fracture mechanics. The smeared crack concept was used, together with a rotating crack model based on total strain; see TNO (2002). The deformation of one crack was smeared out over one element; i.e. the crack band width was chosen to be about the size of one element, estimated from the area of the element. For the elements at the symmetry line, the crack band width was set to twice the size of the elements, due to the symmetry. The hardening in compression was described by the expression of Thorenfeldt *et al.*, as described in TNO (2002). The compressive behaviour was assumed to be uninfluenced by lateral cracking, while lateral confinement of the concrete was assumed to increase the compressive strength and ductility according to the model by Selby and Vecchio. For the tension softening, the curve by Hordijk *et al.* was chosen, see Figure 6. For further description of the used models, see TNO (2002).

The in-situ cast concrete was assumed to be of Swedish class K35. According to the Swedish code, the characteristic compressive strength for this class is 25 MPa. The average compressive strength was calculated according to CEB (1993) as the characteristic value plus 8 MPa, and was thus 33 MPa. This value was used in the analyses. The precast concrete was of class K40, and its average compressive strength was evaluated correspondingly to 36.5 MPa. Other necessary material data for the concrete were estimated according to the expressions in CEB (1993) from  $f_{cc}$  and the maximum aggregate size, which was assumed to be 16 mm. The values used are shown in Table 1.

Table 1 Values used for the concrete in the analyses.

	$f_{cc}$ [MPa]	$f_{ct}$ [MPa]	$E_C$ [GPa]	$G_F$ [N/m]
in-situ cast concrete	33	2.56	32.1	69.2
precast concrete	36.5	2.80	33.2	74.3

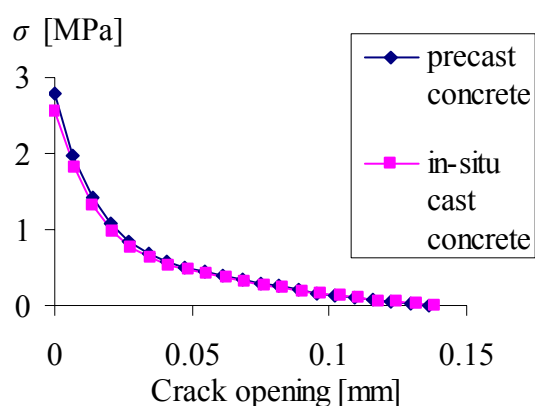


Figure 6 Stress versus crack opening used as input for the concrete.

## 2.2.2 Reinforcement

The constitutive behaviour of the reinforcement and steel was modelled by the Von Mises yield criterion with associated flow and isotropic hardening. The reinforcement was assumed to have an elastic modulus of 200 GPa and a yield strength of 700 MPa.

## 2.2.3 Interaction between concrete and reinforcement

Slip is allowed between the reinforcement and the concrete. They are assumed to interact with a bond versus slip correlation according to CEB (1993), assuming unconfined concrete and “other” bond conditions, see Figure 7.

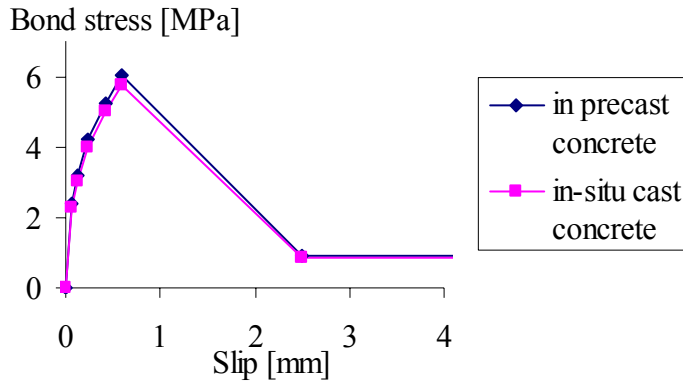


Figure 7 Bond versus slip correlation used as input for the interaction between the concrete and the reinforcement.

## 2.2.4 Interaction between precast and in-situ cast concrete

The modelling of the interaction between the precast and the in-situ cast concrete is of large importance for the results of the analyses. The surface is intended to be combed by a steel rake in the production, to avoid a too smooth surface. The interface was modelled by the use of a friction model, assuming a certain cohesion, see Figure 8. This means that a certain amount of shear stresses could be carried without any normal stresses applied; however the possibility to carry shear stresses increases with increasing amount of normal stresses. As can be seen in Figure 8, two important parameters in this model are the cohesion,  $c$ , and the coefficient of friction,  $\mu$ . Other parameters needed in the model is the dilatation parameter,  $\eta$ , and the elastic stiffnesses  $D_{11}$  and  $D_{22}$ . The dilatation parameter,  $\eta$ , describes how large normal stresses that are created during slip if normal deformations are prevented, or how large normal deformations that will take place during slip if no normal stress is present. It should be chosen larger or equal to zero, which corresponds to that slip will not cause any normal stresses; and smaller or equal to the coefficient of friction (else energy will be created). The stiffnesses  $D_{11}$  and  $D_{22}$  describes the relation between the stresses and the deformations in the elastic range;  $D_{11}$  for the stress and the deformation in the normal direction, and  $D_{22}$  for the shear stress and slip. Preliminary analyses of the lap splice showed that the choice of input for the interaction between the precast and the in-situ concrete is very important; therefore they were specially investigated.

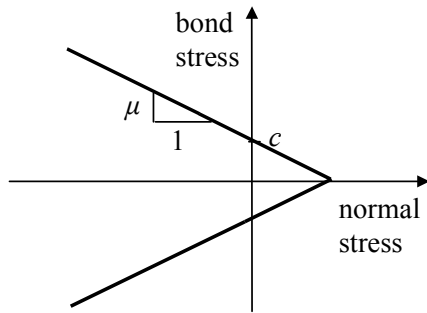


Figure 8 Friction model used for the interface between the precast and the in-situ cast concrete.

First of all, information about the two most important parameters, the cohesion,  $c$ , and the coefficient of friction,  $\mu$ , were searched for. In fib (1998), guide lines for the shear capacity of the interface between precast and in-situ concrete are given. There, the following design equation is given:

$$\tau = c + \mu \cdot (\sigma + \rho f_{yd}) \quad (1)$$

where  $\tau$  is the shear stress

$c$  is the cohesion, see Figure 8.

$\mu$  is the coefficient of friction, see Figure 8.

$\sigma$  is the normal stress acting on the interface, in this equation taken as positive when in compression while the opposite is valid in Figure 8.

$\rho$  is the amount of reinforcement crossing the interface.

This equation is intended for use in analytical models, with reinforcement crossing the interface equally distributed over the area. In the cast joint investigated here, the reinforcement crossing the interface is not equally distributed – in some cases there is no reinforcement at all, and in some, there is only one reinforcement bar on the whole length. Therefore, this equation was not used to take the effect of the reinforcement into account. However, the design values of the cohesion and the coefficient of friction given in fib (1998) were considered to be of use for the modelling of the cast joint. Since the surface should be combed by a steel rake, design category 2 should apply, however, also the values recommended for design category 1 were tested, to study the influence of the surface. The values of the cohesion are calculated from the compressive strength of the concrete; here the concrete with the smallest compressive strength was used. The values obtained in this way are listed in Table 2.

The design values of the cohesion and the coefficient of friction were also compared with what was measured in an experimental investigation, Nissen *et al.* (1986). They measured larger values, both for the cohesion and the coefficient of friction, for a surface which was combed by a steel rake, see Table 2.

Table 2 Values of the cohesion and the coefficient of friction for the interface between the precast and the in-situ cast concrete.

	$c$ [MPa]	$\mu$ [-]
fib (1998), design category 1	0.29	0.6
fib (1998), design category 2	0.58	0.9
Nissen <i>et al.</i> (1986), experimental	1.69	1.54

No information was found in the literature about the dilatation parameter,  $\eta$ , and the elastic stiffnesses  $D_{11}$  and  $D_{22}$ . Preliminary analyses showed that even if the influence on the results of these parameters was not as large as for the first two parameters, still it was not negligible. To find reasonable values of these parameters, and to check how the effect of the reinforcement crossing the cast joint could be modelled, some of the tests of Nissen *et al.* (1986) were modelled. These analyses are described in section 3. After this calibration, the dilatation parameter  $\eta$  was chosen to 0.1, and the elastic stiffnesses  $D_{11}$  and  $D_{22}$  were chosen to  $1 \cdot 10^{12}$  N/m<sup>3</sup> and  $1 \cdot 10^{11}$  N/m<sup>3</sup>, respectively.

### 3 Finite element analyses of joints between precast and in-situ concrete

#### 3.1 Finite element models

Preliminary analyses of the lap splice showed that the interaction between the precast and the in-situ concrete is very important for the behaviour; therefore the modelling of this interaction was specially investigated. Nissen *et al.* (1986) made a large experimental investigation on the interaction between precast and in-situ concrete. In their investigation, the type of surface, normal stress, and the amount of reinforcement crossing the joint were varied. Here, their tests that had surfaces that were combed by a steel rake were modelled, since that is the type of surface which is intended to be used in the present application. Nissen *et al.* (1986) carried out 12 tests without reinforcement, and 12 tests with reinforcement (all with the same amount of reinforcement). The test set-up used is shown in Figure 9.

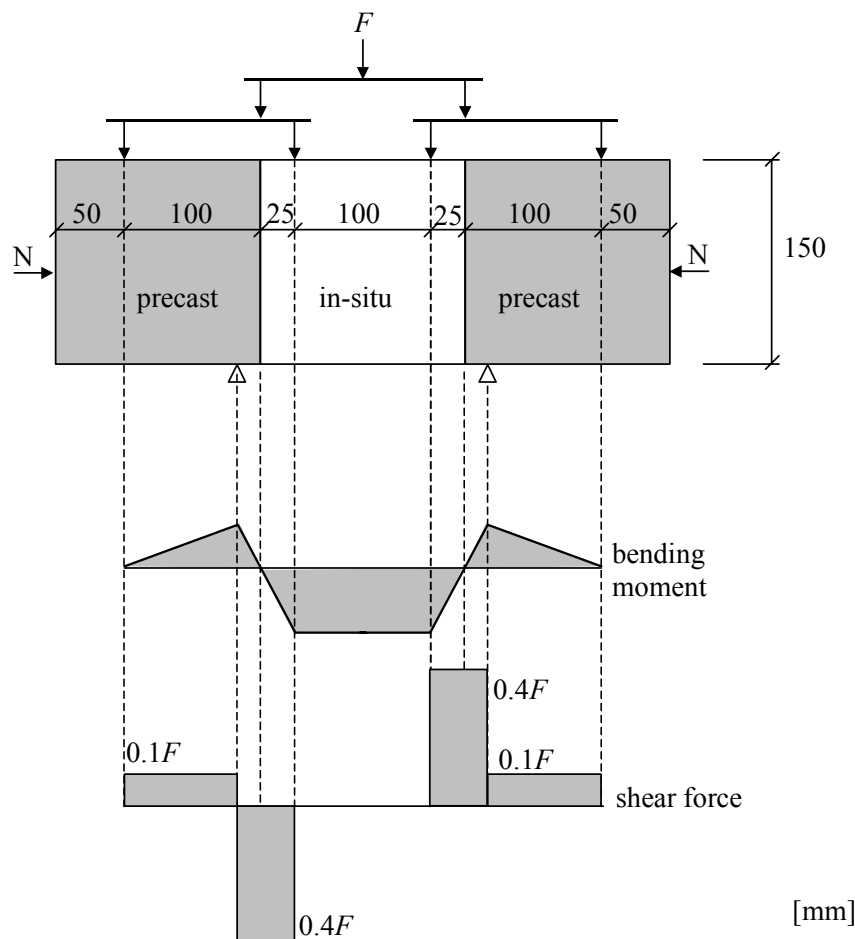


Figure 9 Test set-up used by Nissen *et al.* (1986) to investigate the interaction between precast and in-situ concrete. The depth of the test specimens were 150 mm.

The finite element model used for the analyses of these tests is shown in Figure 10. Two-dimensional modelling was used, assuming plane stress, using the symmetry line in the middle of the test specimen. The concrete was modelled with four-node quadrilateral elements. The cast joint was modelled by the use of interface elements, with separate nodes for the precast and the in-situ cast concrete.

The nodes around the loaded and supported nodes were tied to that node, as shown in Figure 10, in order to avoid local crushing of the concrete. When a normal force was applied in the analyses, the left side was forced to have the same deformation. Loading was applied on a loading beam, which was very stiff. When no normal pressure was applied, the loading was deformation controlled, while it was load controlled when a normal pressure was applied in order to keep a constant ratio between the shear and the normal stresses.

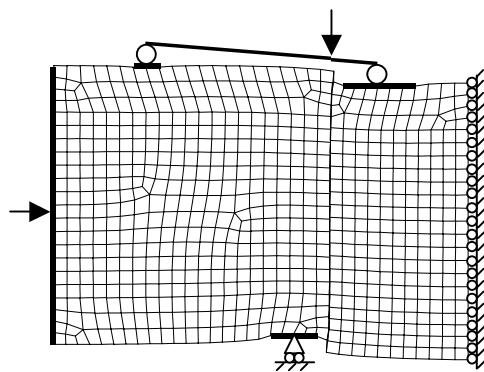


Figure 10 Deformed mesh used in the analyses of the tests of Nissen et al. (1986).

In the tests including reinforcement, there were two closed stirrups, i.e. four reinforcement bars that crossed the interface. Only half the thickness of the interface was modelled, and the reinforcement bars were modelled with beam elements with a circular cross-section. The positioning of the reinforcement is shown in Figure 11. Interface elements were used between the concrete and the reinforcement, describing a bond-slip relation. Across the cast joint, a very short beam element was used for the reinforcement. For that short element, no interface element to the concrete was used, as it was passing the interface of the cast joint, see Figure 11.

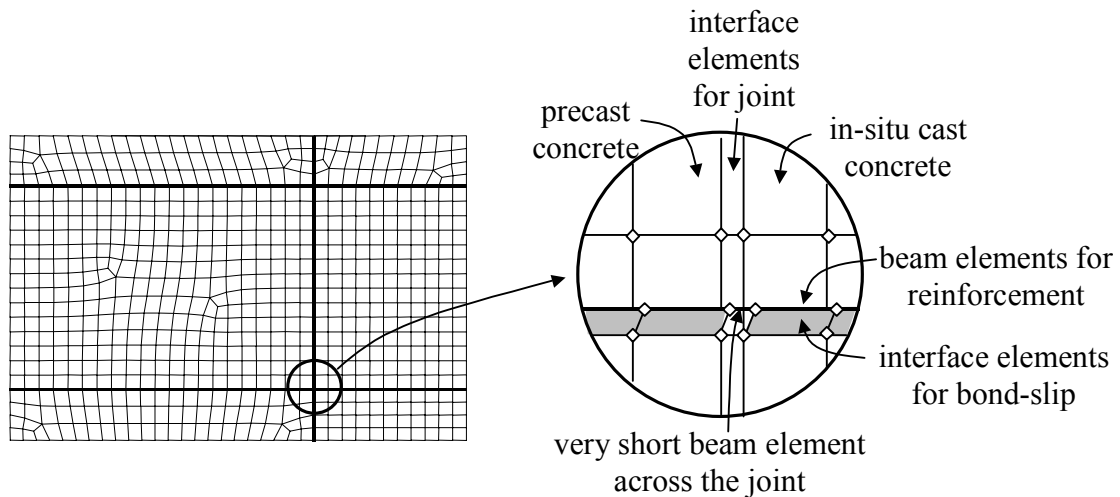


Figure 11 Positioning of the reinforcement, and detail of the model where the reinforcement crossed the cast joint.

The materials were modelled similarly as in the analyses of the lap splices, see section 2.2. The values used for the concrete in these analyses are listed in Table 3. The reinforcement in the analyses had an elastic modulus of 200 GPa, a yield strength of 546 MPa, and an ultimate strength of 853 MPa at a strain of 0.1. The yield strength and the ultimate strength were measured values, while the elastic modulus and the ultimate strain were assumed values. The bond versus slip correlation used for the interaction between the reinforcement and the concrete is shown in Figure 12.

Table 3 Values used for the concrete in the analyses of the tests of Nissen et al. (1986).

	$f_{cc}$ [MPa]	$f_{ct}$ [MPa]	$E_C$ [GPa]	$G_F$ [N/m]
in-situ cast concrete	20.0	1.57	27.1	48.7
precast concrete	30.0	2.36	31.1	64.7

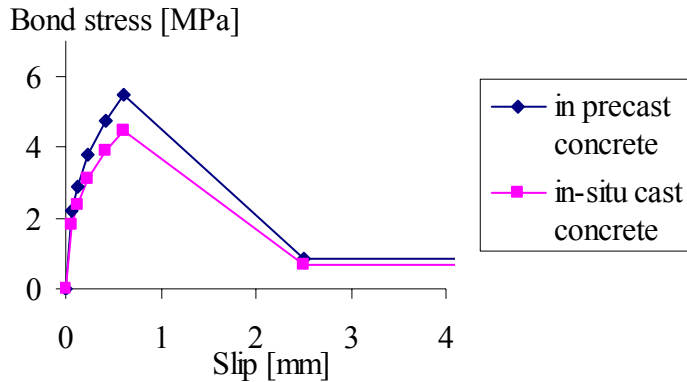


Figure 12 Bond versus slip correlation used as input for the interaction between the concrete and the reinforcement in the analyses of the tests of Nissen *et al.* (1986).

### 3.2 Calibration of the parameters of the joint

The interface between the precast and the in-situ concrete was modelled by the use of a friction model, assuming a certain cohesion, as described in section 2.2.4. From the experimental results of Nissen *et al.* (1986), it was very clear that a friction model was a reasonable choice. Values of the two most important parameters in the friction model, i.e. the cohesion,  $c$ , and the coefficient of friction,  $\mu$ , could be directly derived from the tests without any reinforcement, to 1.69 MPa and 1.54 respectively.

When a too small value of the elastic stiffness  $D_{11}$  was chosen, the in-situ cast concrete penetrated into the precast concrete to a large degree, and the failure was not obtained in the joint as it was in the tests. To avoid this,  $D_{11}$  was increased to a value of  $1 \cdot 10^{12}$  N/m<sup>3</sup>. The elastic stiffness  $D_{22}$  describes the initial stiffness in a bond stress versus slip curve. Since this was very large in the experiments,  $D_{22}$  was chosen to be  $1 \cdot 10^{11}$  N/m<sup>3</sup>.

An initial value of the dilatation parameter,  $\eta$ , was estimated to 0.1. The reason for this choice is that for friction behaviour it is reasonable to assume less dilatation than the upper limit, which is when the dilatation parameter is set to the coefficient of friction, see Jirásek (1993) for a discussion. Smaller and larger values of the dilatation parameter were tried. In Figure 13, the bond stress versus slip for the unreinforced joint without any normal stress is shown, for various dilatation parameters. The experimental results indicate the measured scatter; the descending part was not stable in the tests. As can be seen, the capacity increases too much when a larger dilatation parameter is used; the descending branch then also becomes unstable. The two analyses with the dilatation parameter set to zero and 0.1 gives here similar results. However, when looking at the corresponding results for the joint with reinforcement and a normal stress present, see Figure 14, it is shown that a dilatation parameter of zero gives an underestimation of the capacity of the joint. Accordingly, it was concluded that the choice of the dilatation parameter to 0.1 appears to be a reasonable choice.

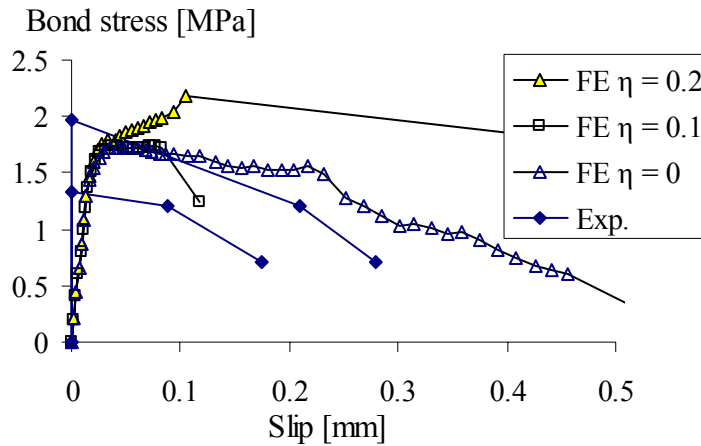


Figure 13 Bond stress versus slip for the unreinforced joint without any normal stress, results from analyses where the dilatation parameter was varied. Experimental results from Nissen et al. (1986).

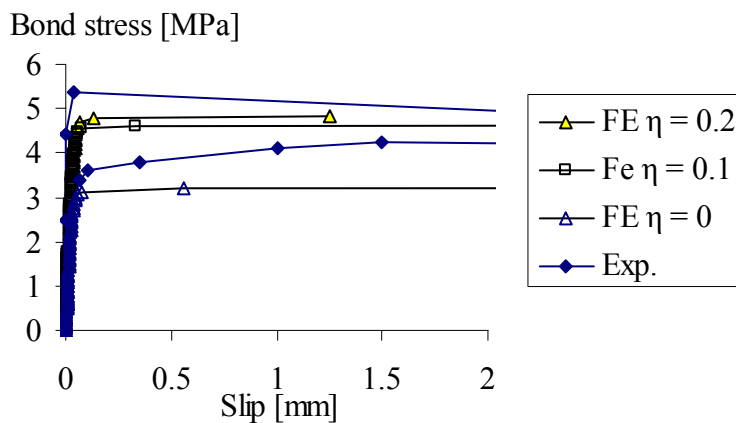


Figure 14 Bond stress versus slip for the reinforced joint; results from analyses where the dilatation parameter was varied. The bond stress divided by the normal stress was 3.0 in the analyses, and varied between 2.8 to 3.2 in the tests. Experimental results from Nissen et al. (1986).

The maximum obtained bond stresses in tests and analyses without reinforcement are compared in Figure 15, where also the line for the cohesion and coefficient of friction given as input is shown. As can be seen, the results correspond well. As long as the failure mode is in the joint, it is expected that the results will coincide with the input. The slightly lower maximum bond stress in the analysis with a high normal stress depends on that in that analysis, crushing of the concrete at the support occurred.

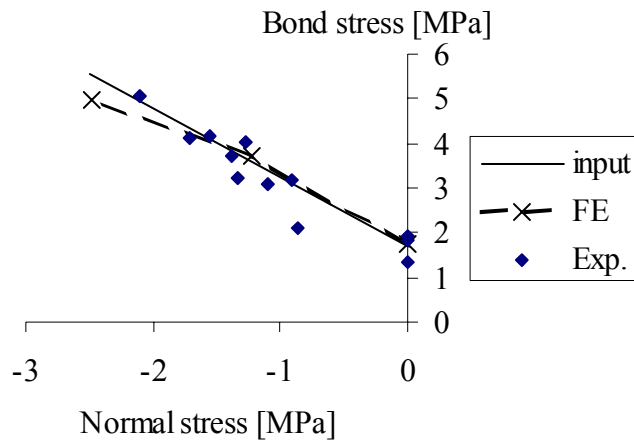


Figure 15 Maximum obtained bond stress versus normal stress in tests and analyses without reinforcement. Input data for the analyses is also shown. Experimental results from Nissen et al. (1986).

The maximum obtained bond stresses in tests and analyses with reinforcement are compared in Figure 16, where also the line for the cohesion and coefficient of friction given as input is shown. As can be seen, the reinforcement causes an increase in capacity, which appears to be rather well described in the analyses.

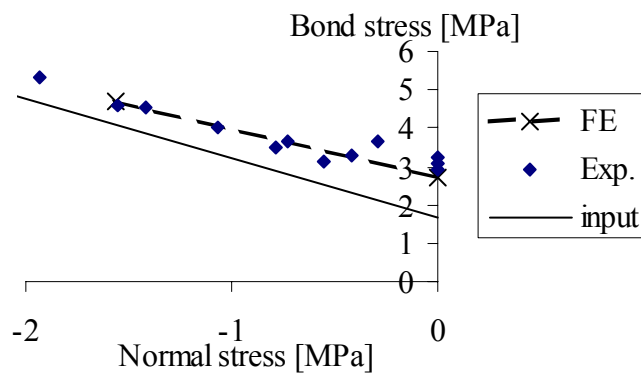


Figure 16 Maximum obtained bond stress versus normal stress in tests and analyses with reinforcement. Input data for the joint in the analyses is also shown. Experimental results from Nissen et al. (1986).

## 4 Results of analyses of a lap splice in a lattice girder system

One “normal case” of a lap splice in a lattice girder system was modelled, for geometry *etc.* see section 2. The cohesion and coefficient of friction in the joint was in the “normal case” assumed to be according to fib (1998), design category 2. The welds in the reinforcement mesh were considered as described in section 2.1, and there was no bent reinforcement that crossed the joint. With this “normal case” as a starting point, the following variations were also modelled:

- With different values of the cohesion and the coefficient of friction in the interface between the precast and the in-situ cast concrete, see Table 2.
- Without considering the welds in the reinforcement mesh.
- With bent reinforcement crossing the cast joint.
- With lower yield strength of the transverse reinforcement.
- Without welds and with lower yield strength of the transverse reinforcement.

### 4.1 Normal case

In the analysis of the normal case, the reinforcement did not reach yielding; the maximum obtained stress in the reinforcement was 659 MPa. The bending moment per meter along the lattice girder versus the rotation at the loaded end is shown in Figure 17. In the same graph, the moment calculated to cause yielding of the reinforcement (42.6 kNm/m) is indicated. Furthermore, the crack pattern at the maximum load is shown in Figure 18. The first peak, denoted A, in the moment versus rotation diagram corresponds to when the crack in the in-situ concrete over the joint between the lattice girder elements appears (at the symmetry line, to the right in Figure 18). At the next small peak, B, the second crack appears, which is the crack second closest to the symmetry line. The location of this crack is controlled by the location of the welds in the reinforcement mesh. The third crack from the right in Figure 18 is located at the position of the next weld in the reinforcement mesh. This crack starts to develop at a rotation of about  $3.5 \cdot 10^{-3}$ , point C, when also the crack at the loaded end develops. At the maximum load, D, the cast joint between the precast concrete and the in-situ concrete opens up, as can be seen in Figure 19. As there is no reinforcement crossing the joint, the analysis becomes unstable, and in reality, a brittle failure can be expected. It can be noted that almost all the deformation takes place in the two cracks closest to the symmetry line.

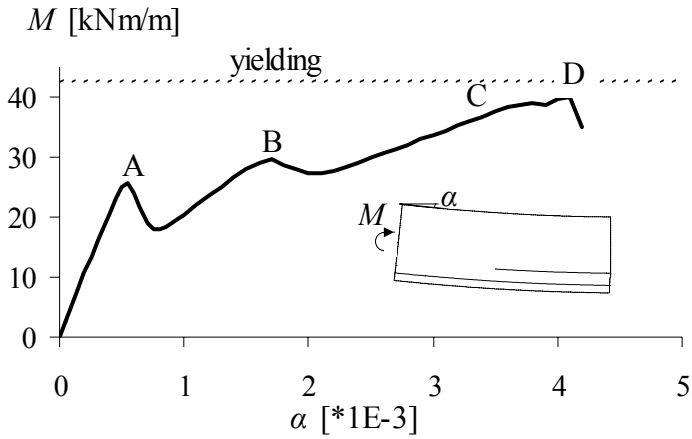


Figure 17 Moment versus rotation at the loaded end obtained in the analysis of the normal case.

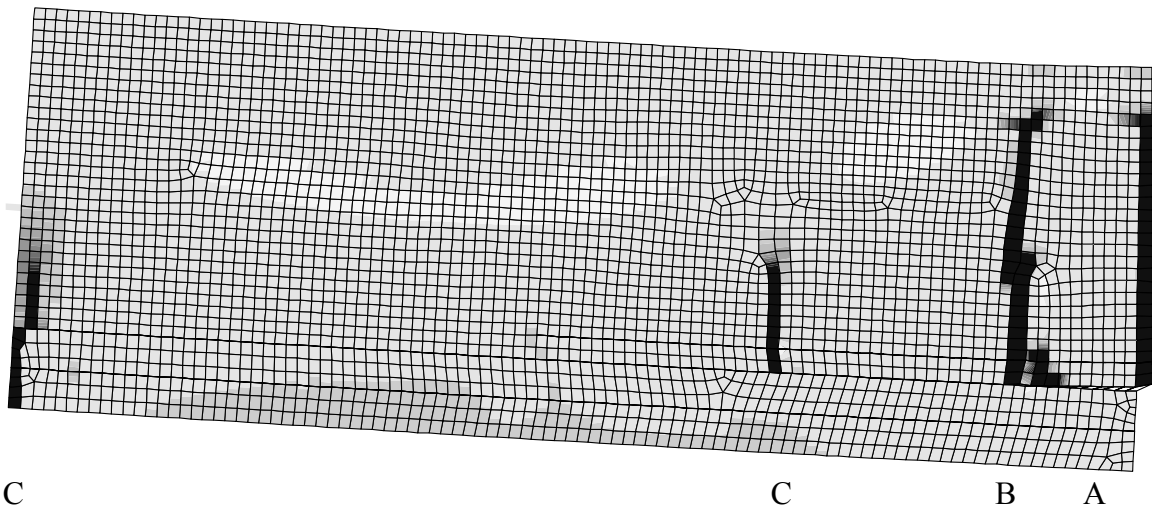


Figure 18 Deformed mesh at maximum load for the normal case; dark regions indicate cracks.

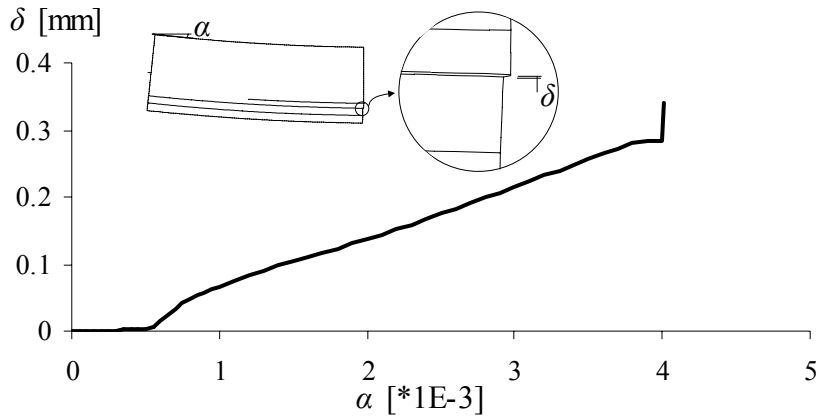


Figure 19 Opening of the cast joint versus rotation at the loaded end obtained in the analysis of the normal case.

In Figure 20, the opening of the joint in the horizontal direction is compared with the crack opening in the in-situ concrete. The opening of the joint in the horizontal direction is obtained from the deformation of the upper node in the precast concrete, while the crack opening in the in-situ concrete is obtained from the deformation over the cracked element. First of all, it can be noted that the crack opening is rather large, meaning that the concrete does not transfer any tensile stresses already for a rather low rotation. Furthermore, the difference in the openings correspond to slip in the cast joint. As can be seen, this starts increasing at a rotation of about  $1.5 \cdot 10^{-3}$ .

In Figure 21, the stress in the reinforcement in the in-situ cast concrete at maximum load is shown. The jumps in this graph correspond to the transfer of stresses due to the welds in the reinforcement mesh. In Figure 22, the deformations in the cast joint at maximum load are plotted versus the  $x$ -coordinate. Again, there are sudden changes at the positions of the welds in the reinforcement mesh.

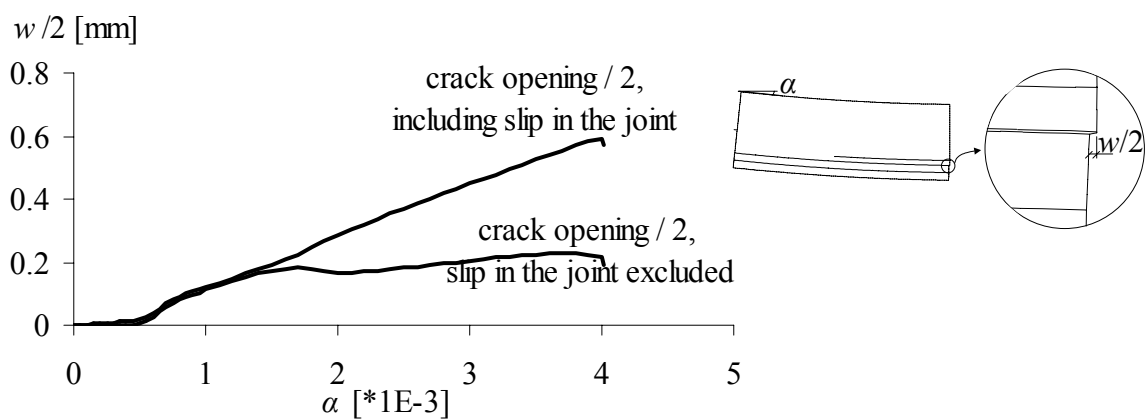


Figure 20 Crack opening at the joint versus rotation at the loaded end obtained in the analysis of the normal case.

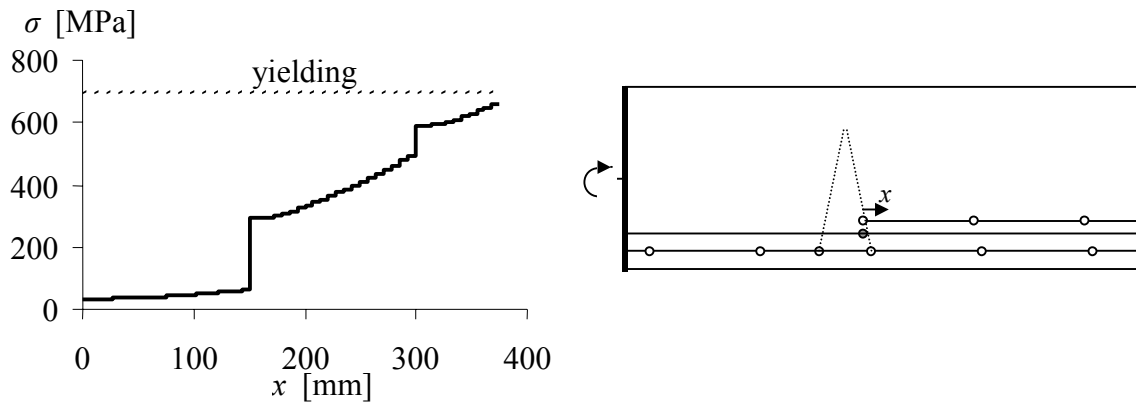


Figure 21 Stress in the reinforcement in the in-situ cast concrete, at maximum load in the analysis of the normal case.

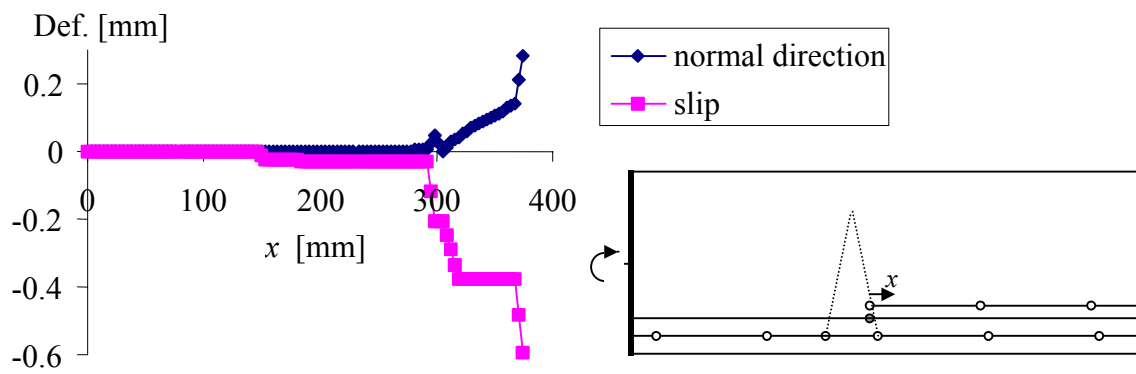


Figure 22 Deformations in the cast joint at maximum load in the analysis of the normal case.

## 4.2 With lower values of the cohesion and the coefficient of friction

Also the design category 1 according to fib (1998) was examined. As this corresponds to a smoother surface than design category 2, which was considered to be the normal case, the cohesion and the coefficient of friction were decreased for the interface between the precast and the in-situ concrete, see Table 2. In this analysis, the maximum obtained stress in the reinforcement was 532 MPa. The bending moment per meter along the lattice girder versus the rotation at the loaded end is shown in Figure 23 and the crack pattern at the maximum load is shown in Figure 24. The cracks appear in the same order as in the analysis of the normal case. Also the failure mode, with opening of the cast joint between the precast concrete and the in-situ concrete is the same. The only difference is that it appears at a lower load, due to the lower capacity of the joint.

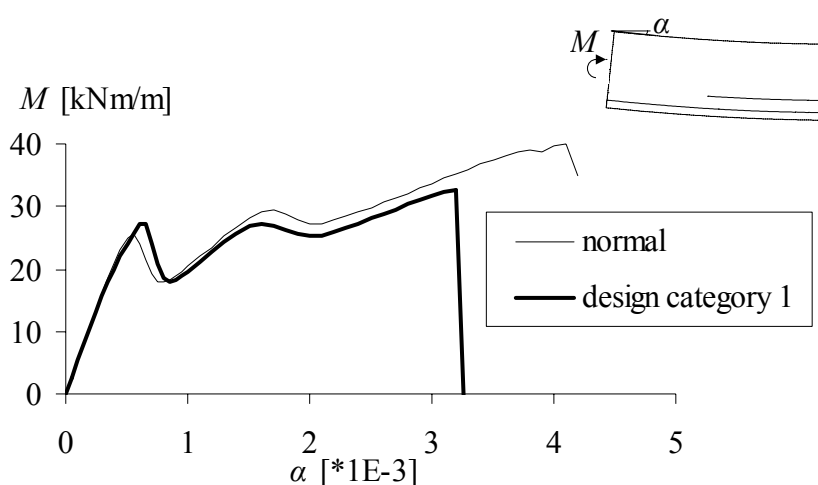


Figure 23 Moment versus rotation at the loaded end obtained in the analysis where design category 1 was assumed for the interface between the precast and the in-situ concrete.

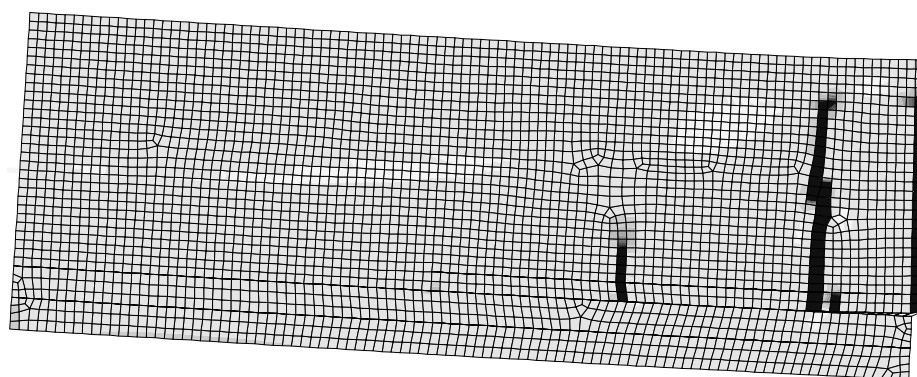


Figure 24 Deformed mesh at maximum load for in the analysis where design category 1 was assumed for the interface between the precast and the in-situ concrete; dark regions indicate cracks.

### 4.3 With higher values of the cohesion and the coefficient of friction

The experiments of joints by Nissen *et al.* (1986) showed higher values of the cohesion and the coefficient of friction than is recommended in fib (1998), see Table 2. The higher values correspond perhaps better to what can be expected in reality. Therefore, an analysis using these values was carried out. In this analysis, the maximum obtained stress in the reinforcement was 655 MPa. This is slightly less than in the analysis of the normal case; however, the behaviour was slightly stiffer, as can be seen in Figure 25. The crack pattern at the maximum load is shown in Figure 26. The cracks appear in the same order as in the analysis of the normal case. Also the failure mode, with opening of the cast joint between the precast concrete and the in-situ concrete is the same.

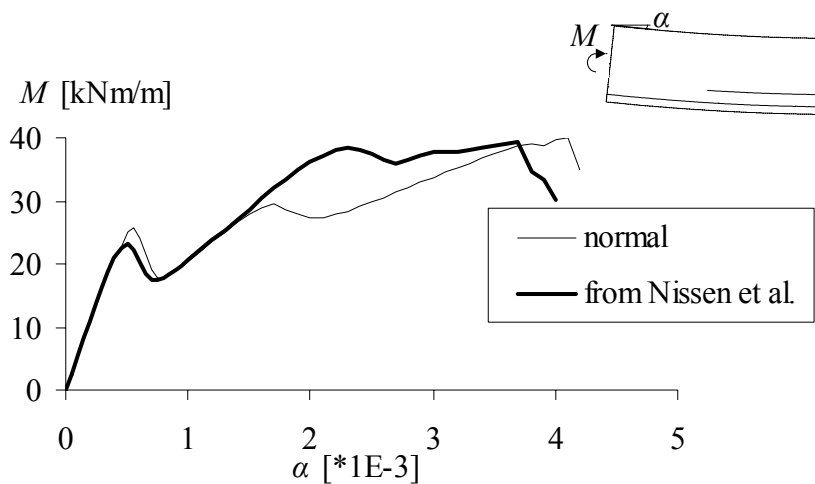


Figure 25 Moment versus rotation at the loaded end obtained in the analysis where the values obtained in Nissen *et al.* (1986) were assumed for the interface between the precast and the in-situ concrete.

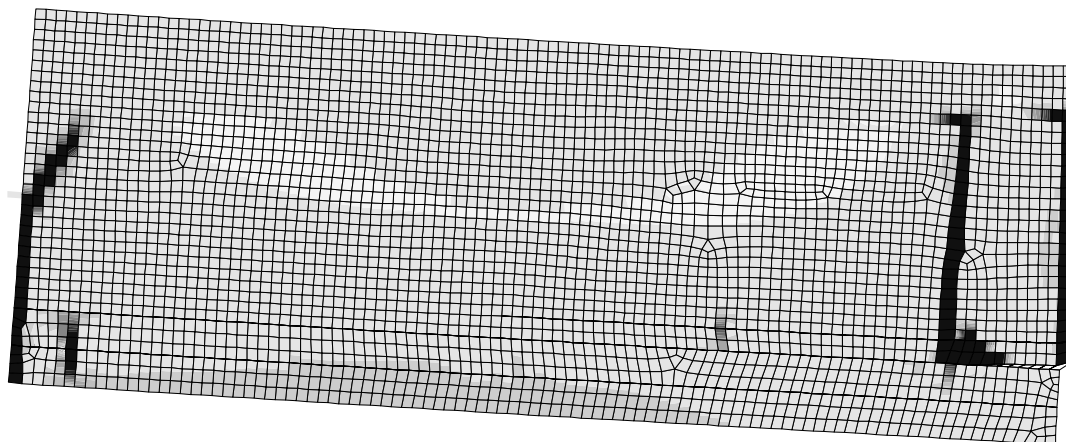


Figure 26 Deformed mesh at maximum load for in the analysis where the values obtained in Nissen *et al.* (1986) were assumed for the interface between the precast and the in-situ concrete; dark regions indicate cracks.

## 4.4 Without considering the welds in the reinforcement mesh

The welds in the reinforcement mesh were in the normal case modelled with tyings, as described in section 2.1. These tyings strongly influence the crack pattern, as does the mesh in reality. One analysis was carried out, where these tyings were taken out, corresponding to a situation with ribbed bars instead of a mesh. The capacity in this analysis increased compared with the normal case: the reinforcement reached yielding at the maximum load, i.e. the maximum stress in the reinforcement was 700 MPa. However, the failure mode was not yielding of the reinforcement; again it was opening of the cast joint between the precast concrete and the in-situ concrete that limited the capacity. The moment versus rotation at the loaded end is shown in Figure 27 and the crack pattern at the maximum load is shown in Figure 28. The first crack is also in this analysis the crack in the in-situ concrete over the joint between the lattice girder elements, corresponding to the first peak in the moment versus rotation diagram. The next peak corresponds to cracking at the loaded end, when the rotation is around  $4.0 \cdot 10^{-3}$ . At maximum load, a crack at the lattice girder truss appears, which is hardly visible in Figure 28. This crack grows in the subsequent steps. Also in this analysis, the failure mode appears to be opening of the the cast joint between the precast concrete and the in-situ concrete, as can be seen in Figure 29.

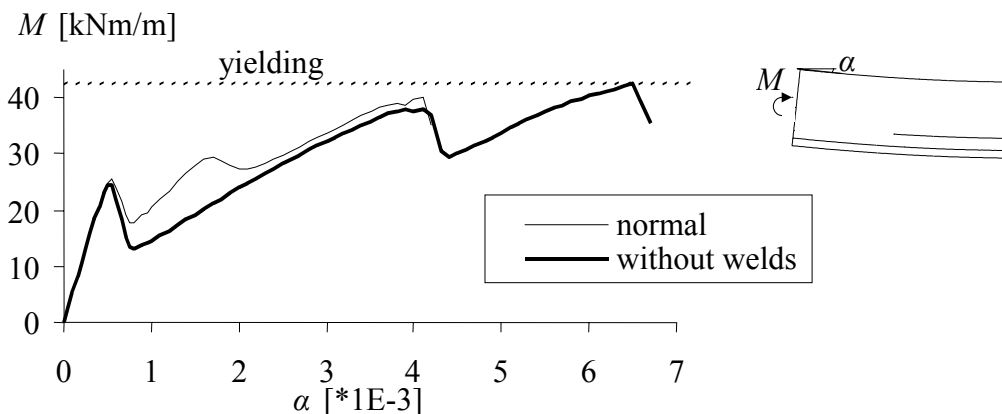


Figure 27 Moment versus rotation at the loaded end obtained in the analysis without welds.

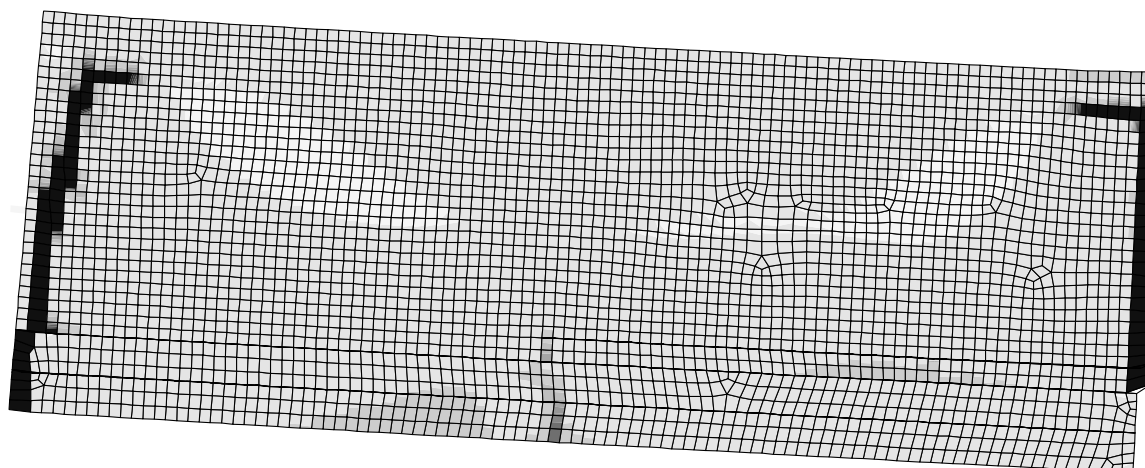


Figure 28 Deformed mesh at maximum load in the analysis without welds; dark regions indicate cracks.

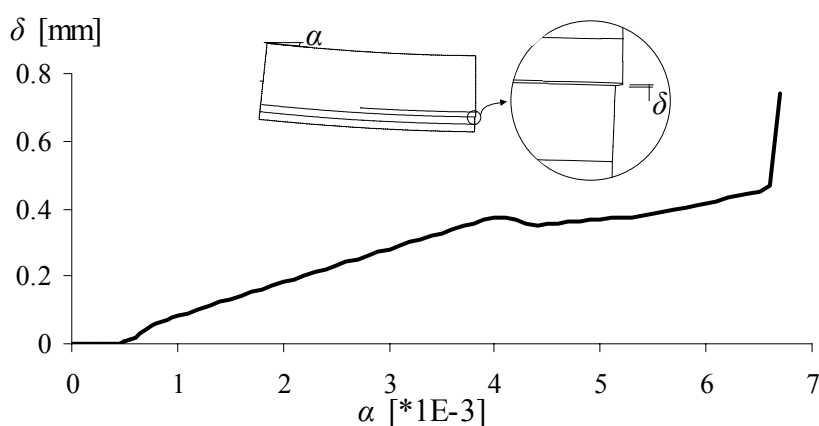


Figure 29 Opening of the cast joint versus rotation at the loaded end obtained in the analysis without welds.

In Figure 30, the opening of the joint in the horizontal direction is compared with the crack opening in the in-situ concrete. As can be seen, the slip in the joint is much smaller in this analysis than it was in the normal case, compare Figure 20. In Figure 31, the stress in the reinforcement in the in-situ cast concrete at maximum load is shown. Again, there is a large difference in the behaviour compared to the normal case (Figure 21); as there are no welds transferring stresses, the stress in the reinforcement is here increased smoothly along the length. In Figure 32, the deformations in the cast joint at maximum load are plotted versus the  $x$ -coordinate. As can be seen, the deformations in the joint are very small, except for very close to the crack at the joint.

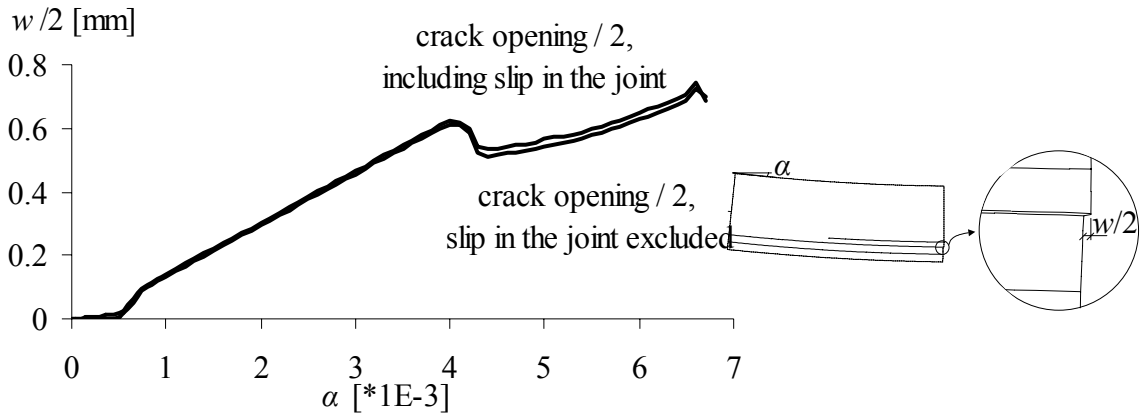


Figure 30 Crack opening at the joint versus rotation at the loaded end obtained in the analysis without welds.

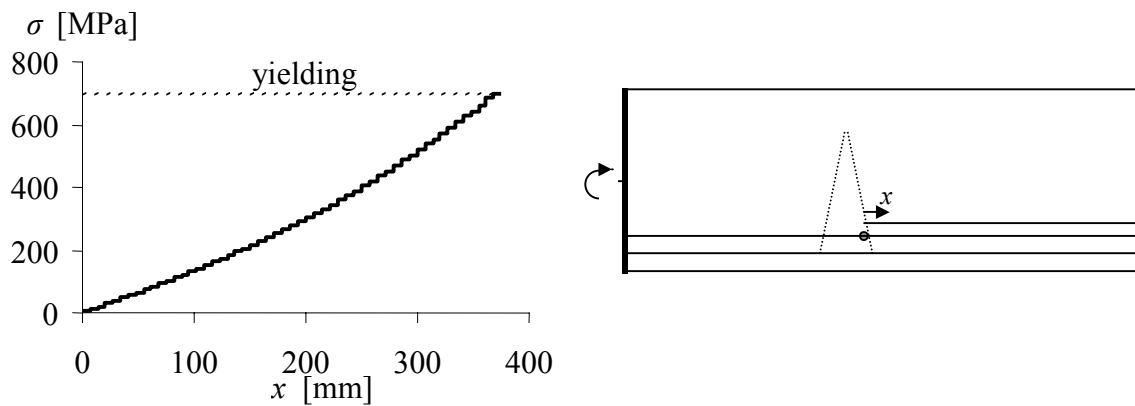


Figure 31 Stress in the reinforcement in the in-situ cast concrete, at maximum load in the analysis without welds.

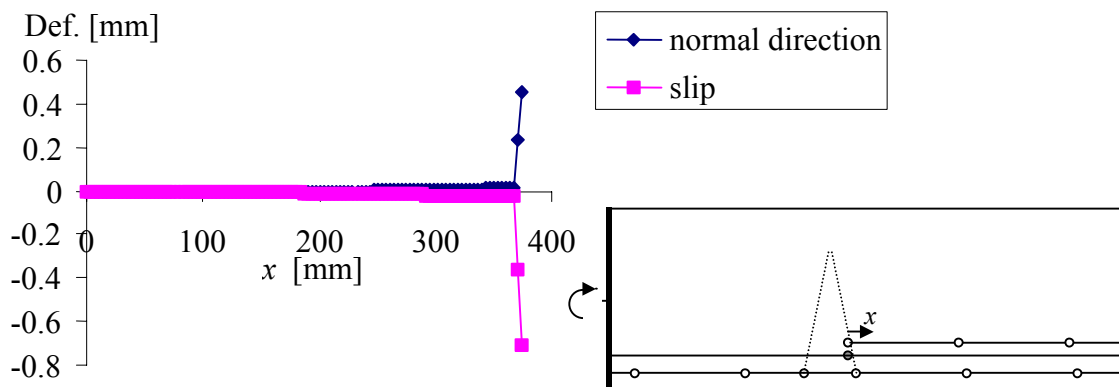


Figure 32 Deformations in the cast joint at maximum load in the analysis without welds.

## 4.5 With bent reinforcement crossing the cast joint

The possibility to put bent reinforcement crossing the cast joint was investigated. As a starting point, reinforcement with a diameter of 8 mm at a distance 150 mm with a yield strength of 500 MPa was used. The placement of the bent reinforcement is shown in Figure 33.

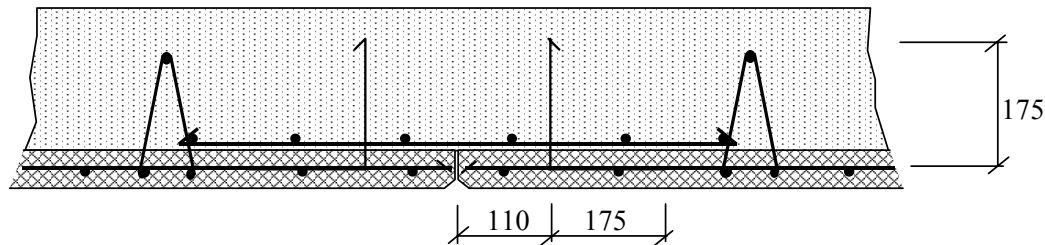


Figure 33 Placement of the bent reinforcement.

In the analysis with bent reinforcement crossing the cast joint, the reinforcement reached yielding at the maximum load, i.e. the maximum stress in the reinforcement was 700 MPa. However, the failure mode was not yielding of the reinforcement, but also for this case it was opening of the cast joint between the precast concrete and the in-situ concrete that limited the capacity. The deformation capacity was, however, approximately doubled compared to the normal case. The moment versus rotation at the loaded end is shown in Figure 34 and the crack pattern at the maximum load is shown in Figure 35.

The first crack is also in this analysis the crack in the in-situ concrete over the joint between the lattice girder elements, corresponding to the first peak in the moment versus rotation diagram, A. At the next small peak, B, the second crack appears, which is the crack second closest to the symmetry line. The location of this crack is controlled by the location of the welds in the reinforcement mesh. The third crack from the right in Figure 35 is located at the position of the next weld in the reinforcement mesh. This crack starts to develop at a rotation of about  $3.5 \cdot 10^{-3}$ , point C, when also the crack at the loaded end develops. At point D, the crack at the lattice girder truss appears, but only in the lower part of the cross-section, in the precast concrete. At the same time, the second crack at the loaded end develops. At this point, the analysis without reinforcement crossing the joint (the normal case) fails. However, in the analysis where the bent reinforcement is included, it is possible to increase the load after a sudden drop. One more peak is obtained at point E, when the crack at the lattice girder truss spreads also to the in-situ cast concrete. Thereafter, the load is increased until yielding of the reinforcement occurs just before the maximum load. The cast joint between the precast concrete and the in-situ concrete opens up very fast in the analysis, see Figure 36, and the reinforcement crossing the joint gets very large stresses. The analysis becomes unstable. The stress in the bent reinforcement where it crosses the cast joint is shown in Figure 37. As beam elements was used for this reinforcement, the stress differs over the reinforcement, i.e. it carries a small bending moment. As can be seen, there are rather small stresses, until the final load step, when bending in the other direction compared to the earlier steps occurs. This is when the joint suddenly opens up.

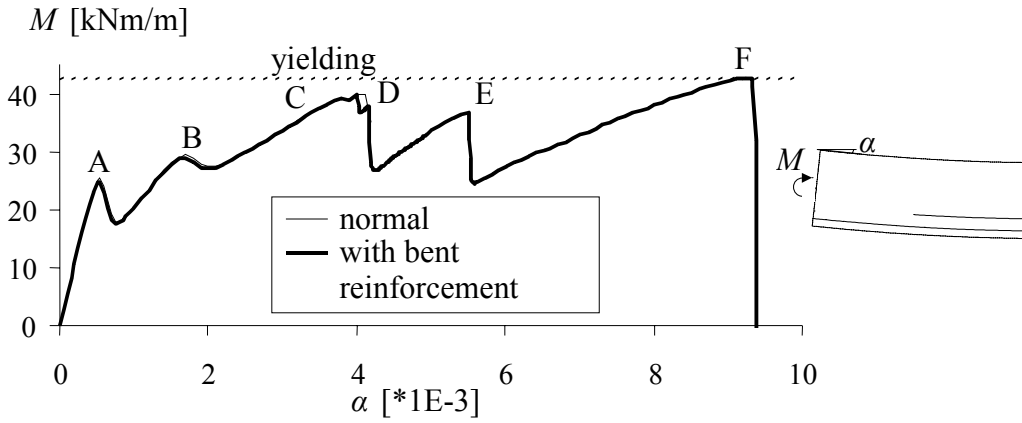


Figure 34 Moment versus rotation at the loaded end obtained in the analysis with bent reinforcement crossing the cast joint.

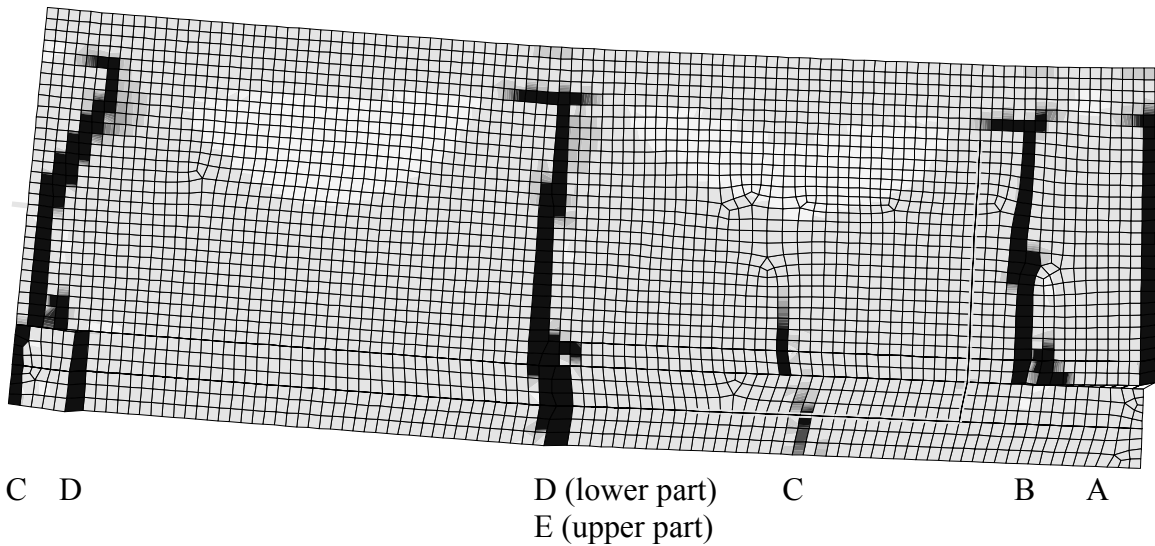


Figure 35 Deformed mesh at maximum load in the analysis with bent reinforcement crossing the cast joint; dark regions indicate cracks.

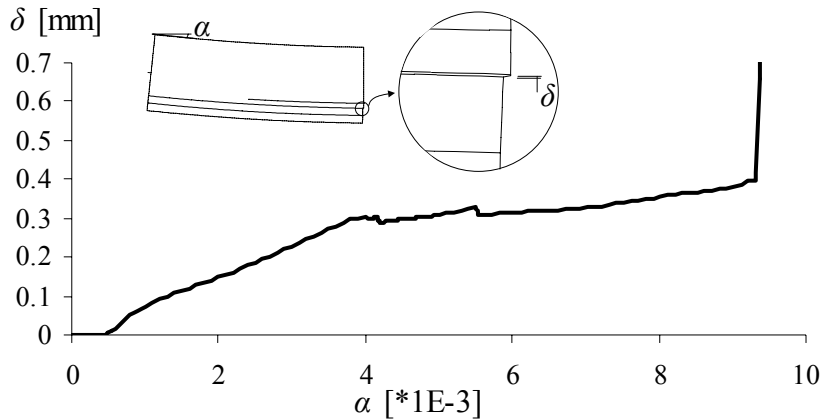


Figure 36 Opening of the cast joint versus rotation at the loaded end obtained in the analysis with bent reinforcement.

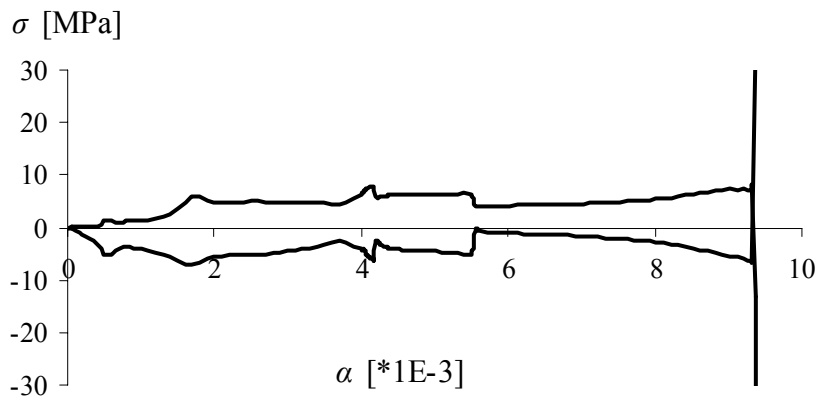


Figure 37 Stress in the bent reinforcement where it crosses the cast joint.

#### 4.6 With bent reinforcement crossing the cast joint close to the joint

When looking at the results from the analysis including bent reinforcement crossing the cast joint, it was assumed that the instability in the end was at least partly due to the distance between the bent reinforcement and the joint. By putting the bent reinforcement closer to the joint, it was believed that the reinforcement would get larger stresses at an earlier stage of the loading, and that this would result in a more stable opening of the joint. The placement of the bent reinforcement shown in Figure 38 was therefore investigated. Also in this analysis, reinforcement with a diameter of 8 mm at a distance 150 mm with a yield strength of 500 MPa was used.

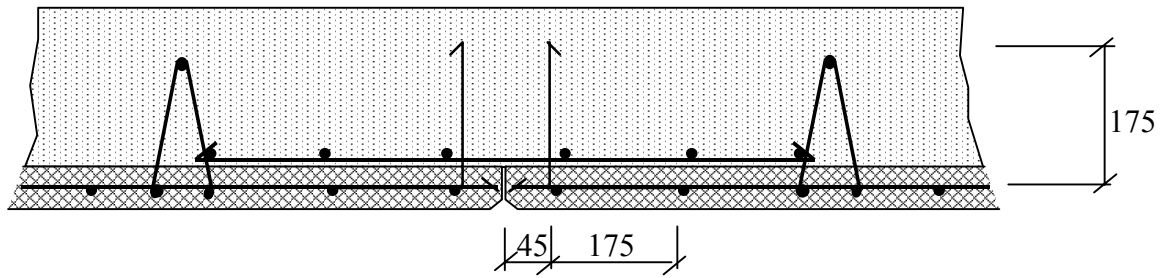


Figure 38 Placement of the bent reinforcement close to the joint.

The moment versus rotation at the loaded end is shown in Figure 39 and the crack pattern at the maximum load is shown in Figure 40. As can be seen, this analysis becomes unstable even for smaller rotations than the normal case. Cracking around the bent reinforcement starts when the rotation is about  $2.0 \cdot 10^{-3}$ , and at maximum load, the joint opens up. The stress in the bent reinforcement where it crosses the cast joint is shown in Figure 41. As can be seen, the stresses are a lot larger than when the bent reinforcement was placed further away from the joint (compare Figure 37), with yielding already at a rotation slightly smaller than  $3.0 \cdot 10^{-3}$ . In the final load step, when the analysis becomes unstable, bending in the other direction compared to the earlier steps occurs.

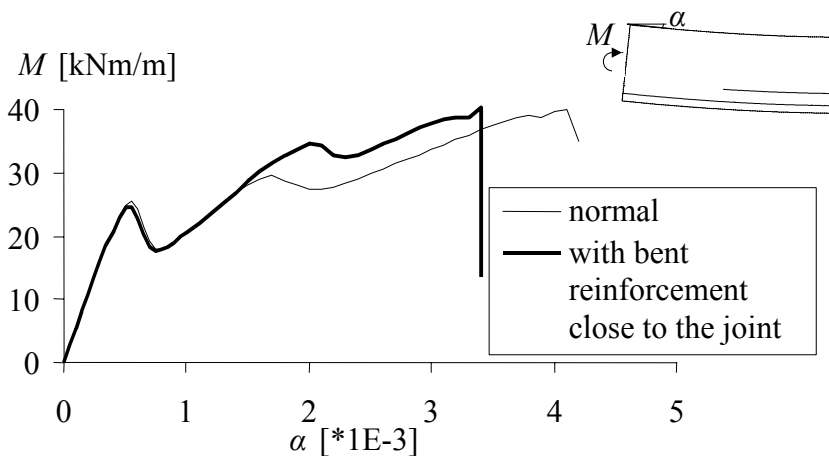


Figure 39 Moment versus rotation at the loaded end obtained in the analysis with bent reinforcement close to the joint.

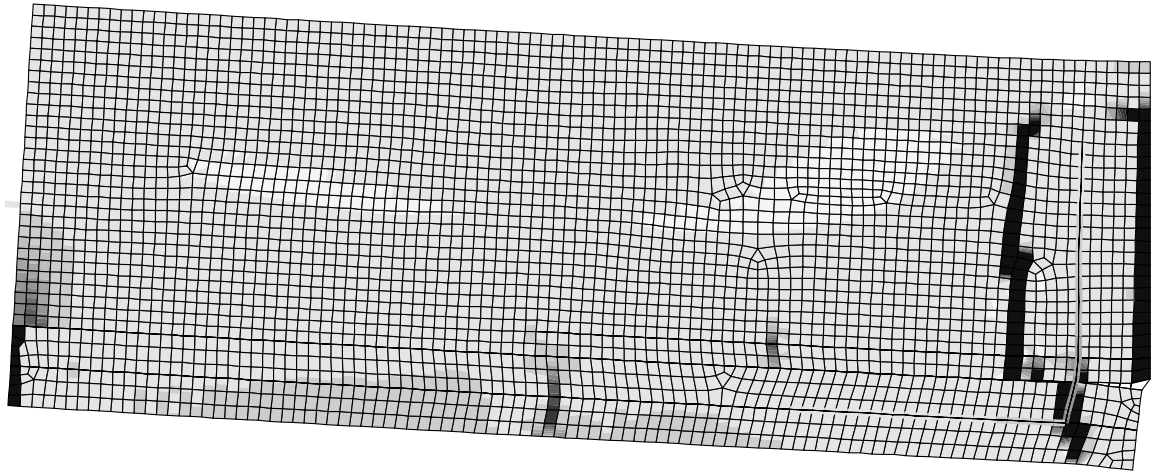


Figure 40 Deformed mesh at maximum load in the analysis with bent reinforcement close to the joint; dark regions indicate cracks.

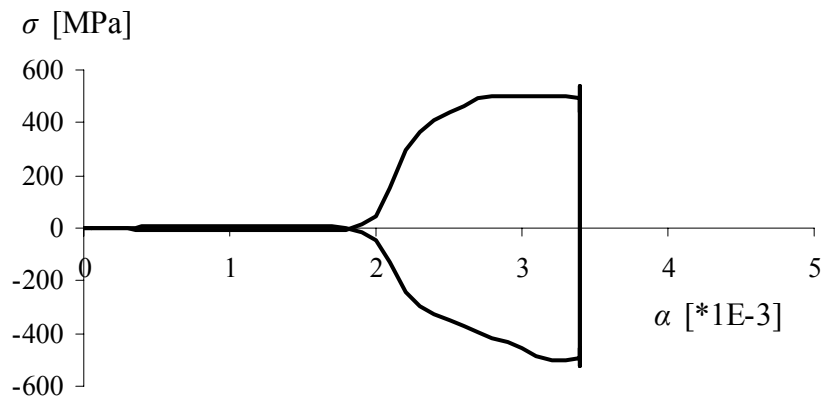


Figure 41 Stress in the bent reinforcement where it crosses the cast joint, in the analysis with the bent reinforcement close to the joint.

## 4.7 With lower yield strength of the reinforcement

When looking at the results from all of the analyses, the reinforcement reached yielding in some of them, but it was not possible to keep this yield force in any of the analyses. To investigate what would happen if the reinforcement has a lower yield strength, one analysis was run where the yield strength of the transverse reinforcement was reduced to 500 MPa. Other input was chosen as in the normal case. The moment versus rotation at the loaded end is shown in Figure 42 and the crack pattern at the maximum load is shown in Figure 43. As can be seen, the reinforcement in this analysis reaches yielding, and it is possible to keep this yielding moment some additional rotation before the joint opens up.

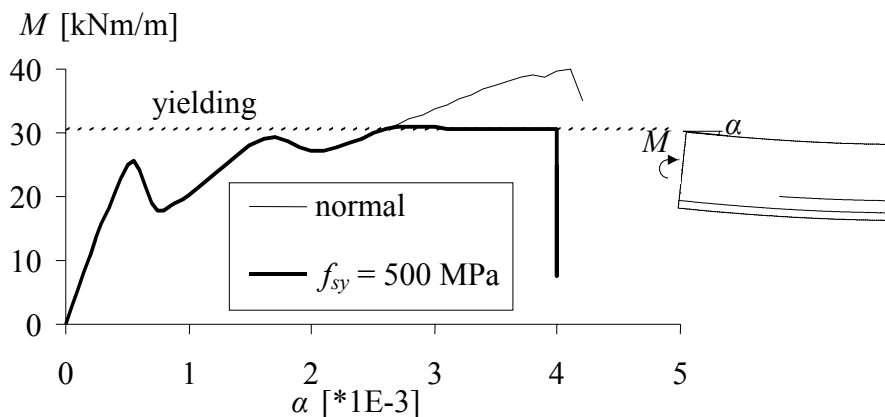


Figure 42 Moment versus rotation at the loaded end obtained in the analysis with reduced yield strength of the transverse reinforcement.

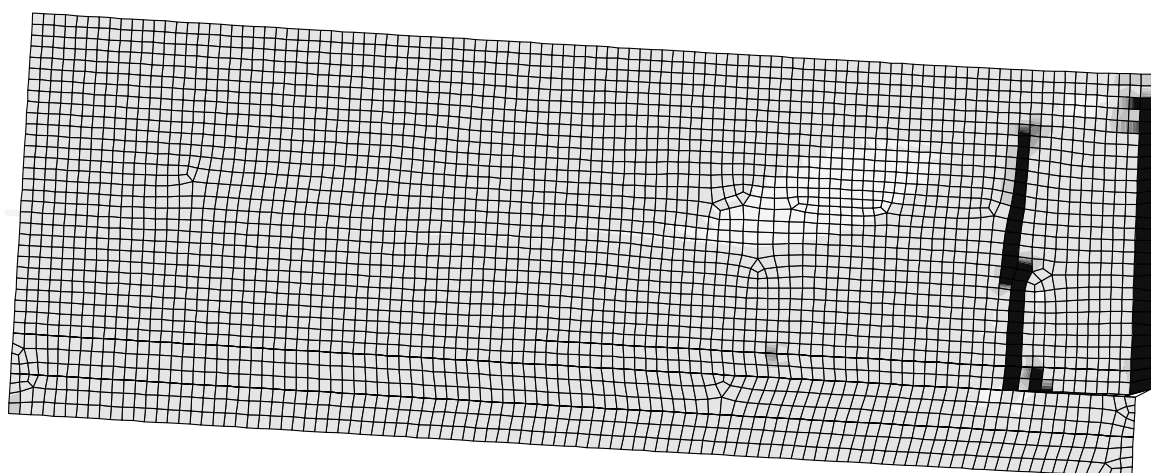


Figure 43 Deformed mesh at maximum load in the analysis with reduced yield strength of the transverse reinforcement; dark regions indicate cracks.

## 4.8 Without welds and with lower yield strength of the reinforcement

One analysis where the welds of the reinforcement mesh were not taken into account, combined with a yield strength of the transverse reinforcement of 500 MPa was carried out. Other input was chosen as in the normal case. The moment versus rotation at the loaded end is shown in Figure 44 and the crack pattern at the maximum load is shown in Figure 45. Also in this analysis, opening of the cast joint limited the capacity, as can be seen in Figure 46. However, the reinforcement in this analysis reached yielding, and the deformation capacity was in this analysis rather large, larger than when the welds of the reinforcement mesh was taken into account. In this case, all the deformation is taken at the crack at the symmetry line. In the analysis, the reinforcement element closest to the symmetry line is the only one that reaches yielding, i.e. the yield penetration is only about 7 mm. In reality, the yield penetration would be larger, which is of importance for the deformation capacity. The reason for this difference between analysis and reality is that in the analysis, the loss of bond between reinforcement and concrete when the reinforcement is yielding is not taken into account. In order to do that, a more sophisticated model needs to be used for the bond mechanism.

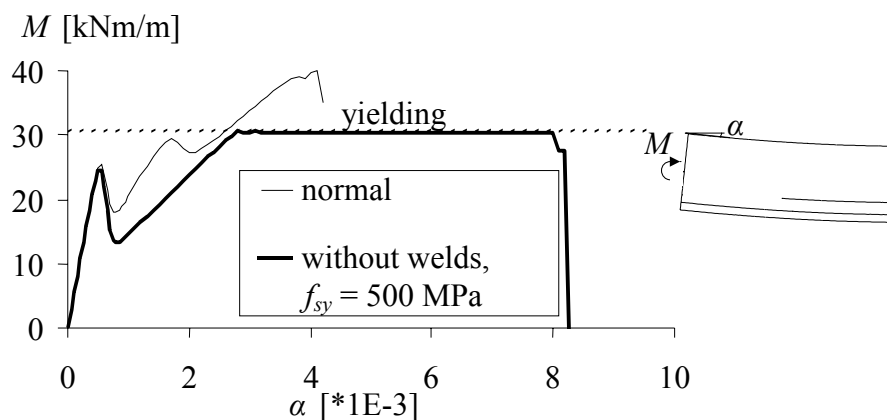


Figure 44 Moment versus rotation at the loaded end obtained in the analysis without welds and with reduced yield strength of the transverse reinforcement.

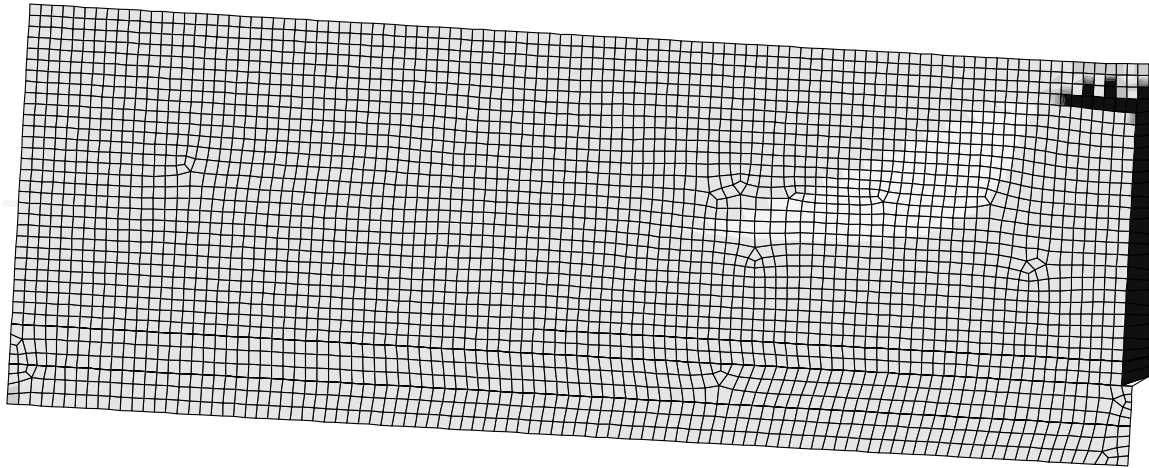


Figure 45 Deformed mesh at maximum load in the analysis without welds and with reduced yield strength of the transverse reinforcement; dark regions indicate cracks.

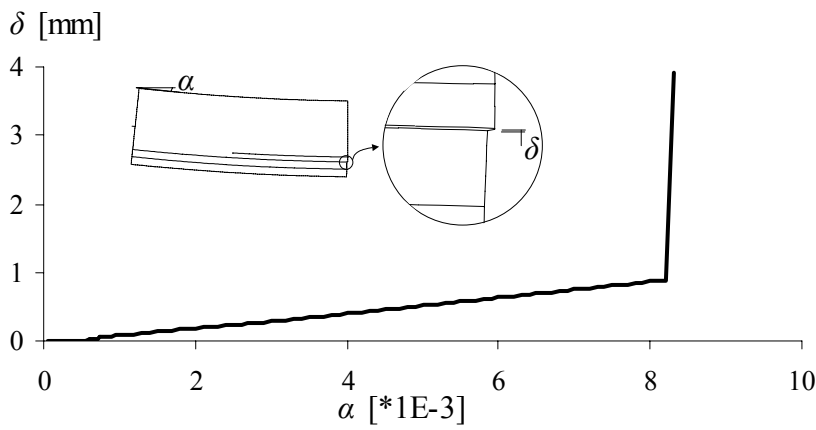


Figure 46 Opening of the cast joint versus rotation at the loaded end obtained in the analysis without welds and with reduced yield strength of the transverse reinforcement.

## 5 Conclusions

In the present study, the possibility to put transverse reinforcement in the precast concrete panels and complement with lapped reinforcement across the joints at the construction site was studied. The behaviour of such a joint, when subjected to bending, was investigated in two-dimensional finite element analyses. The analyses show that the cast joint between the precast concrete and the in-situ cast concrete is the weak link in this detailing, as could be expected. In the analyses where a rather large amount of transverse reinforcement was used,  $\varnothing 8$  s150 NPs 700, the joint could be loaded close to yielding of the reinforcement; then opening of the cast joint occurred in all of the analyses. When no bent reinforcement, crossing the cast joint, is present, the failure mode will most likely become brittle. It is therefore recommended to have bent reinforcement crossing the cast joint. Two analyses were carried out with two different placement of bent reinforcement,  $\varnothing 8$  s150 B500B in both cases. When the bent reinforcement was placed close to the joint, it obtained large stresses rather early in the analysis, and the analysis became unstable for rather low rotations. When the bent reinforcement was placed further away from the joint, the transverse reinforcement reached yielding, and the deformation capacity was approximately doubled compared to the other analyses.

For small amounts of transverse reinforcement, or reinforcement with a lower yield strength, it might be possible to use the studied detailing even without bent reinforcement crossing the joint. In one analysis where the transverse reinforcement had a reduced yield strength, 500 MPa instead of 700 MPa, the reinforcement reached yielding, and it was possible to keep the yielding moment some additional rotation before the joint opened up. However, it must be noted that the roughness of the surface is very important for the behaviour of the studied detailing; if the detailing is intended to be used without bent reinforcement crossing the joint, special care must be taken in order to get a surface which is not too smooth, and to ensure that there is no dust when the in-situ concrete is cast at the construction site.

The analyses including bent reinforcement crossing the cast joint became unstable when the joint opened up. It is uncertain if there would be a brittle behaviour also in reality with this detailing. If so, one possible solution can be to place the reinforcement crossing the cast joint with an inclination as shown in Figure 47. Another possible improvement in detailing could be to have two (or more) bent reinforcement bars on each side of the joint, or to place lattice girders closer to the end.

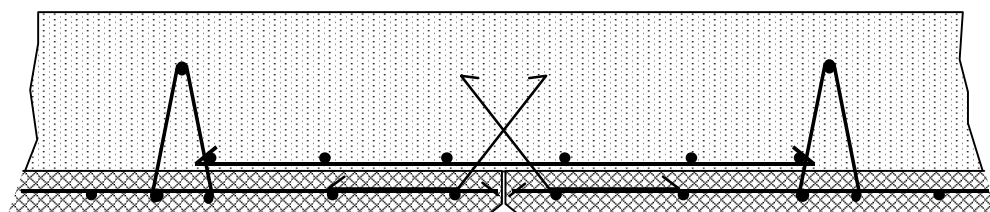


Figure 47 Bent reinforcement crossing the cast joint with an inclination.

In all the analysed cases, except when there was reinforcement crossing the cast joint, the deformations were localised to a small region close to the joint. This might partly be due to the higher capacity of the prefabricated concrete, compared to the in-situ concrete.

The limited rotation capacity of the splices in the analyses is a disadvantage if the behaviour corresponds to reality. Even if the bending moment capacity is enough for design purposes, a certain rotation capacity is needed in order to distribute the bending moments as was assumed in design. The Swedish code, Boverket (1994), does not have any formal requirements of rotation capacity, however, in the European code, there is an indirect requirement through limiting the ratio between the height of the compressive zone and the effective height ( $x/d$ ). It is, however, not straightforward to translate this limit to a required deformation capacity of the studied splice.

It is worth to note that the stresses in the main direction are not included in the modelling, since two-dimensional modelling was chosen. The interface between the precast and the in-situ cast concrete will be used for shear transfer also in the main direction. This will reduce the possibility to transfer shear in the studied direction. This is an important aspect, which most likely needs to be more studied. Another uncertainty in the used model is the total locking of deformations in the cast joint at the lattice girder truss; this might have led to an overestimation of the capacity.

The modelling of the cast joint is of very large importance for the results of the analyses. The modelling of that was checked through analyses of joints between precast and in-situ concrete tested by Nissen et al. (1986), who made a large experimental investigation on the interaction between precast and in-situ concrete. Still some uncertainty about the input parameters remain. Furthermore, long term effects such as shrinkage and creep were not included in these analyses. It is recommended to do further studies, including full-scale testing of lap splices before this detailing is used in practice.

## 6 References

- Boverket (1994): *Boverkets handbok om betongkonstruktioner BBK 94, Band 1 - Konstruktion (Boverket's Handbook for Concrete Structures BBK94, Vol. 1: Design. In Swedish)*, Boverket, Byggavdelningen, Karlskrona, Sweden, 1994.
- CEB (1993): *CEB-FIP Model Code 1990*, Bulletin d'Information 213/214, Lausanne, Switzerland, 1993.
- fib (1998): *Composite floor structures - Guide to good practice*. Fédération internationale du béton, prepared by FIP Commission on Prefabrication.
- Jirásek M. (1993): *Modeling of fracture and damage in quasibrittle materials*. Ph.D. Thesis, Theoretical and Applied Mechanics, Northwestern University, The United States of America, 1993.
- Nissen I., Daschner F. and Kupfer H. (1986): *Versuche zur notwendigen Schubbewehrung zwischen Betonfertigteilen und Ortbeton (Tests of the necessary shear reinforcement between precast concrete elements and in situ concrete. In German)*. Deutscher Ausschuss für Stahlbeton, Berlin.
- TNO (2002): *DIANA Finite Element Analysis, User's Manual release 8.1*, TNO Building and Construction Research, 2002.